Ann Nucl Med (2013) 27:554–563
DOI 10.1007/s12149-013-0719-3

ORIGINAL ARTICLE

The usefulness of ^{18}F-FDG PET/MRI fusion image in diagnosing pancreatic tumor: comparison with ^{18}F-FDG PET/CT

Shigeki Nagamachi · Ryuichi Nishii · Hideyuki Wakamatsu · Youichi Mizutani · Shogo Kiyohara · Seigo Fujita · Shigemi Futami · Tatefumi Sakae · Eiji Furukoji · Shozo Tamura · Hideo Arita · Kazuo Chijiiwa · Keiichi Kawai

Received: 19 September 2012 / Accepted: 17 March 2013 / Published online: 12 April 2013

Abstract
Purpose This study aimed at demonstrating the feasibility of retrospectively fused ^{18}F FDG-PET and MRI (PET/MRI fusion image) in diagnosing pancreatic tumor, in particular differentiating malignant tumor from benign lesions. In addition, we evaluated additional findings characterizing pancreatic lesions by FDG-PET/MRI fusion image.
Methods We analyzed retrospectively 119 patients: 96 cancers and 23 benign lesions. FDG-PET/MRI fusion images (PET/T1 WI or PET/T2WI) were made by dedicated software using 1.5 Tesla (T) MRI image and FDG-PET images. These images were interpreted by two well-trained radiologists without knowledge of clinical information and compared with FDG-PET/CT images. We compared the differential diagnostic capability between PET/CT and FDG-PET/MRI fusion image. In addition, we evaluated additional findings such as tumor structure and tumor invasion.
Results FDG-PET/MRI fusion image significantly improved accuracy compared with that of PET/CT (96.6 vs. 86.6 %). As additional finding, dilatation of main pancreatic duct was noted in 65.9 % of solid types and in 22.6 % of cystic types, on PET/MRI-T2 fusion image. Similarly, encasement of adjacent vessels was noted in 43.1 % of solid types and in 6.5 % of cystic types. Particularly in cystic types, intra-tumor structures such as mural nodule (35.4 %) or intra-cystic septum (74.2 %) were detected additionally. Besides, PET/MRI-T2 fusion image could detect extra benign cystic lesions (9.1 % in solid type and 9.7 % in cystic type) that were not noted by PET/CT.
Conclusions In diagnosing pancreatic lesions, FDG-PET/MRI fusion image was useful in differentiating pancreatic cancer from benign lesions. Furthermore, it was helpful in evaluating relationship between lesions and surrounding tissues as well as in detecting extra benign cysts.

Keywords ^{18}F FDG-PET/CT · ^{18}F FDG-PET/MRI fusion image · Pancreatic tumor

S. Nagamachi (✉) · R. Nishii · H. Wakamatsu · Y. Mizutani · S. Kiyohara · S. Fujita · S. Futami · T. Sakae · E. Furukoji · S. Tamura · H. Arita
Department of Radiology, School of Medicine, Miyazaki University, 5200 Kihara, Kiyotake, Miyazaki-city, Miyazaki Prefecture 889-1692, Japan
e-mail: snagama@med.miyazaki-u.ac.jp

K. Chijiiwa
Department of the 1st Surgery, Faculty of Medicine, Miyazaki University, 5200 Kihara, Kiyotake, Miyazaki-city, Miyazaki Prefecture 889-1692, Japan

K. Kawai
Faculty of Health Science, School of Medicine, Kanazawa University, Kanazawa, Ishikawa Prefecture 920-8640, Japan

Introduction

^{18}F-fluorodeoxyglucose (FDG)-positron emission tomography (PET)/CT is helpful in staging of pancreatic cancer [1–3]. As for differential diagnosis, it is difficult to distinguish pancreatic cancer from various benign lesions of focal FDG uptake such as inflammatory lesion [4]. Standardized uptake value (SUV) of FDG-PET is a ordinary used quantitative index for diagnosing pancreatic cancer. The dual time point evaluation is one of methods for improving diagnostic ability [5, 6]. Still some overlaps exist between malignancy and benign lesions, for example, pancreatic cancer of relatively low SUV values or pancreatitis of high SUV value [7–9]. Therefore, it is difficult

setting optimal SUV cut-off level to differentiate malignancy from benign lesions.

In this regard, ^{18}F-FDG-PET/CT allows precise coregistration of metabolically active lesions and anatomical abnormalities, and it can make up for a drawback of PET [10, 11]. However, the accuracy of ^{18}F-FDG-PET/CT without contrast media in assessing structures of cystic lesion such as intraductal papillary mucinous neoplasm (IPNM) remains inadequate. In addition, diagnosis of local involvement such as main pancreatic duct (MPD) invasion or peri-pancreatic nodal involvement remains inadequate, either. One of reasons for poor performance of FDG-PET/low-dose CT in diagnosing pancreatic lesion is insufficiency in visualizing anatomic border of similar density. Although the breath-hold technique can improve the tumor delineation and also the quantification of SUV measurements [12], it is not always available in the patients with respiratory failure.

MRI is suitable for evaluating boundary between pancreas and surrounding tissues because of its superiority in tissue contrast resolution. Indirect findings associated with cancer invasion, such as pancreatic duct dilatation or collateral veins dilatation, will also be evaluable. In addition, qualitative diagnoses such as necrosis, cystic degeneration or fibrotic changes are possible using MRI [13]. Integrated MR/PET scanners have recently been developed and expected to perform as a new powerful multimodality imaging tool [14–16]. An improved soft tissue contrast provided by MR created different image sets, which may establish better diagnostic tree in various field. However, owing to limited availability of hybrid PET/MRI system, PET/MR fusion images using software are still now used in various lesions [17–20]. Recently, Tatsumi et al. reported that PET/MRI fusion, especially PET with T1WI, is superior to PET/CT in characterizing pancreatic tumors [20]. However, the former study did not address the usefulness in the differential diagnosis of cystic lesion such as benign IPMN or intraductal papillary mucinous carcinoma (IPMC).

The current study was done to investigate the feasibility of utilizing ^{18}F-FDG PET/MRI fusion images to differentially diagnose pancreatic cancer from benign lesions by dividing into solid lesions and cystic lesions. In addition, we evaluated the diagnosability of cancer invasion into pancreatic duct or surrounding structures. Also, we evaluated the diagnosability of detecting further additional lesions.

Materials and methods

Patients

One-hundred and nineteen patients (64 males, 55 females; average age 67.1 years; range 34–85 years) with cytology-proven or biopsy-proven diagnosis of pancreatic lesion were included (Tables 1, 2). The diseases comprised of 75 invasive ductal carcinoma, 12 intraductal papillary-mucinous carcinoma (IPMC), 6 mucinous cyst-adenocarcinoma, 3 malignant endocrine tumor, and 23 benign lesions (14 chronic pancreatitis, 6 benign intraductal papillary mucinous neoplasm (IPMN) and 3 serous cyst-adenoma). In 75 cases of invasive ductal carcinoma, 4 cases were cystic type invasive carcinoma derived from intraductal tumor. Although 8 cases were clinically diagnosed as un-resectable advanced invasive ductal carcinoma based on the preoperative image findings. In 14 cases of chronic pancreatitis, 10 cases were finally diagnosed as mass-forming pancreatitis. Although etiology of other 4 cases was unknown, they were diagnosed as pancreatitis during course observation.

Among cancer patients, 20 cancers were diagnosed to be un-resectable, and 76 patients eventually underwent surgery with a curative intention, although the cancer turned out to be un-resectable in 8 because of intra-operative findings. As for staging by UICC, they were categorized as stage I 13, stage IIA 12, stage IIB 14, stage III 18, and stage IV 39.

Patients fasted for at least 5 h. The blood glucose level, measured just before tracer administration, was <140 mg/dl in all patients. Although 12 patients had diabetes, the control of blood glucose was relatively maintained by drug therapy.

Table 1 Clinicopathological profiles of patients ($n = 119$)

	Mean ± SD (range) or n (%)
Age (years)	67.0 ± 10.5 (34–85)
Gender (M:F)	64:55
Location of lesions	
Head	66 (55.4)
Body	37 (31.1)
Tail	16 (13.4)
Maximum tumor diameter (cm)	3.6 ± 1.8 (1.1–12.0)
SUVmax (early)	7.1 ± 3.8 (2.3–23.9)
SUVmax (delayed)	8.8 ± 4.7 (2.5–28.5)

Table 2 Tumor characteristics ($n = 119$)

Diagnosis	S:C
Malignancy	
Invasive ductal carcinoma	75 (71:4)
Intraductal papillary-mucinous carcinoma	12 (0:12)
Mucinous cyst-adenocarcinoma	6 (0:6)
Malignant endocrine tumor	3 (3:0)
Benign	
Pancreatitis	14 (14:0)
Intraductal papillary-mucinous neoplasm	6 (0:6)
Serous cyst adenoma	3 (0:3)
	119 (88:31)

S solid type, *C* cystic type

Data acquisition and image reconstruction

We performed FDG-PET/CT study using a whole-body PET/CT system (Biograph 16; Siemens/CTI, Knoxville, TN). The CT component of PET/CT corresponds to a 16-slice multi-detector-row spiral CT scanner (sensation 16; Siemens) with a transverse FOV of 500 mm and a spatial resolution greater than 1 mm. The PET component of PET/CT allowing 3-dimensional-only acquisition with a field of view (FOV) of 700 mm in the trans-axial direction and 170 mm in the axial direction. The intrinsic resolution is 4.2 mm full width at half maximum. Whole-body FDG-PET/CT images were obtained using the three-dimensional method 60 min after injection of 185–220 MBq FDG. The images were obtained from the top of the brain to the femur in all patients. We did not use intravenous contrast media.

Low-dose plain CT (40 mAs) images were used for anatomical localization. CT-based attenuation correction used 700-mm extended FOV technology (Auto AC; Siemens). All PET images were reconstructed using iterative algorithms (Fourier rebinning plus attenuation-weighted ordered-subset expectation maximization, 4 iterations, 8 subset, 5-mm Gaussian filter) with CT-based attenuation correction. The data were reconstructed with a 256 × 256 matrix and 3-mm slice thickness. All PET and CT images were transferred to a dedicated workstation (ESOFT4.5, Siemens), from which fused PET/CT images were constructed.

We used the following protocol: all patients fasted for at least 5 h before injection of 185 MBq of ^{18}F-FDG. During the uptake phase of approximately 50 min, the patients remained in a quiet position. The first whole body image was done in a supine position. The imaging time was 15–18 min for each patient. In addition to the conventional PET/CT examination, we added an abdominal imaging of a spot view 30 min after the end of the first whole body imaging.

MRI was performed with either 1.5 T scanner (VANTAGE, Toshiba). As the CT portion of PET/CT was performed without contrast media, non-CE transaxial T1- and T2-weighted images (WI) were used for comparison and for fusion with FDGPET. The following were the imaging parameters: In T1 WI, TR 140 ms, TE 2.4 or 4.8 ms, flip angle 70, 6.0 mm slice thickness/1 mm inter-slice gap. In T2WI, TR 3300 ms, TE 90 ms, flip angle 90, 6.0 mm slice thickness/1 mm inter-slice gap.

Both T1WI and T2WI covering pancreatic lesions were fused with PET image automatically using a dedicated software (Fusion 7D, DX MM FOR WINDOWS. VER.6.1.4, MEDASYS JAPAN). Morphological information including the size and internal structure (cystic or solid) was recorded.

All patients provided written informed consent. This study protocol was approved by the review board of the institution.

Image interpretation

Image interpretations were performed on a dedicated workstation (ESOFT4.5, Siemens), which can display three orthogonal planes for CT, PET, and PET/CT fusion images (sagittal, coronal, and trans-axial) and maximum-intensity-projection (MIP) images. These images were visually assessed for accuracy of fusion and alignment in separate instances by the same nuclear medicine radiologists, who were unaware of the clinical information.

The diagnosis by PET/CT was done by two experienced nuclear medicine specialists according to the following criterion: namely, the lesion was diagnosed as malignant when the localized FDG uptake higher than surrounding normal pancreatic tissue was visually observed [20]. Even if the degree of FDG uptake was faint on the early image, it was defined as malignant when FDG uptake increased on the delayed image. It was defined as benign when there was no apparent FDG uptake, and was considered as chronic pancreatitis when localized FDG uptake was noted in multiple calcifications [21]. Decisions on the findings were reached by consensus.

Each PET/MRI fusion image was interpreted by two well-trained radiologists without knowledge of clinical information. The diagnosis of pancreatic cancer was determined when following findings were noted on PET/MRI fusion images: namely, there were irregular shaped solid mass with or without FDG uptake. In cystic tumor, existence of FDG uptake component was diagnosed as malignancy. In addition, existence of mural nodule matched criteria with or without FDG uptake. Even if there was FDG uptake, we diagnosed it as benign when we could not detect any apparent mass or following indirect findings indicating malignancy. Namely, abrupt interruption of main pancreatic duct (MPD) due to tumor accompanying smooth dilation of tail side duct was considered as positive finding [22]. In contrast, multifocal strictures and dilatations of MPD and dilatation of the side-branches, so called 'beaded appearance', were considered to be findings suggestive of chronic pancreatitis [23].

As for invasion to surrounding vasculatures, it was diagnosed by following findings: (1) encasement or occlusion of vessel, with or without collaterals (2) infiltration of tumors to peri-vascular fat tissue (3) circumferential contact of more than 180° between the tumor and the vessel, and (4) mass effect along one side of the vessel for more than 2 cm [24–27]. Invasion on CBD was diagnosed by the dilatation of CBD [28, 29]. Similarly, invasion to adjacent GI tract was diagnosed by the finding indicating broad contact to tumor with irregularity of GI tract contour [29].

Finally, the image findings were carefully correlated to surgical and pathologic records. Then, following issues were evaluated: (1) comparison of diagnostic capabilities

between PET/CT and PET/MRI fusion image (Differential diagnosis of primary lesion). Diagnostic capabilities included sensitivity (Sen), specificity (Spe), positive-predictive value (PPV), negative-predictive value (NPV), and accuracy (ACC). Regarding PET/MRI fusion images, we considered the diagnosis correct if either PET/MRI-T1WI or PET/MRI-T2WI diagnosed them correctly. (2) Comparison of the frequency of additional information, such as intra-tumor structure, relationship between tumor and surrounding tissues and additional lesions, among PET/CT, PET/MRI-T1W I, and PET/MRI-T2WI.

All subjects were divided into solid lesions and cystic lesions and were evaluated, respectively, regarding above issues. Based on intra-operative and pathological findings, the detectability of cancer invasions to GI tract, CBD, and vessels were compared between PET/CT and PET/MRI fusion images.

Table 3 Comparison of diagnostic capability between PET/CT and PET/MRI fused image (differential diagnosis)

	Sens.	Spec.	PPV	NPV	Acc.
PET/CT (total) ($n = 119$)	96.9	43.5	87.7	76.9	86.6
PET/MRI (total) ($n = 119$)	99.0	82.6***	96.9†	95.2	96.6*
PET/CT (solid) ($n = 88$)	97.4	21.4	86.7	60.0	85.2
PET/MRI (solid) ($n = 88$)	98.7	92.9††	98.7*	92.9	97.7**
PET/CT (cystic) ($n = 31$)	95.5	77.8	91.3	87.5	90.3
PET/MRI (cystic) ($n = 31$)	100.0	77.8	91.7	100.0	93.5

Results are expressed in %

* $P = 0.005$, ** $P = 0.004$, *** $P = 0.003$

† $P = 0.003$, †† $P = 0.002$

Statistical analysis

Methods were compared on a per-lesion basis. Diagnostic characteristics (Sens., Spec., PPV, NPV and Acc), were analyzed using the McNemar test (Sen, Spe, ACC) and Chi square test (PPV, NPV). A P value of less than 0.05 was considered to be a statistically significant difference. Statistical analyses were performed with statistical software Stat Flex (Version 6.0, Artech, Osaka, Japan).

Results

In comparing diagnostic capabilities between PET/CT and PET/MRI fusion images, the latter demonstrated significant better Acc (86.6 vs. 96.6 %). Similarly, both Spec. and PPV significantly improved (43.5 vs. 82.6 % and 87.7 vs. 96.9 %) (Table 3). Twelve of 119 cases (10.0 %) were diagnosed correctly based only on morphological diagnosis by PET/MRI fusion images.

In the analysis of solid type tumor, Acc was significantly better in PET/MRI fusion images compared with that of PET/CT images (85.2 vs. 97.7 %). Spec. and PPV of PET/MRI fusion images also improved significantly compared with those of PET/CT images (21.4 vs. 92.9 %, 86.7 vs. 98.7 %). As for the cystic lesion, there was no statistical significance between PET/MRI fusion image and PET/CT.

As additional findings, intra-tumor structure such as internal septum (74.2 %) or mural nodule (35.4 %) was frequently noted on PET/MRI-T2 fusion image (Table 4). In particular, presence of mural nodule was diagnostic finding suggesting malignancy with or without uptake of FDG (Figs. 1, 2). Multilocular structure was also often recognized by PET/MRI-T2

Table 4 Additional findings detected by PET/CT and PET/MRI fusion images

	Solid type ($n = 88$)			Cystic type ($n = 31$)		
	(PET/CT)	(Tl)	(T2)	(PET/CT)	(Tl)	(T2)
Infra-tumor structures						
Mural nodule	–	–	–	0.0	12.9	35.4
Internal septum	–	–	–	0.0	22.6	74.2
Internal or adjacent structures						
Dilatation or irregularity of MPD	6.8	22.7	65.9	9.7	9.7	22.6
Encasement of adjacent vessels	8.0	11.4	43.1	0.0	0.0	6.5
Narrowing of CBD	0.0	9.0	22.7	0.0	0.0	3.2
Adhesion to GI tract	5.7	12.5	15.9	0.0	0.0	0.0
Additional benign lesion						
Cyst	0.0	0.0	9.1	0.0	0.0	9.7

(%)

(T1) PET/MRI-T1 fusion image, *(T2)* PET/MRI-T2 fusion image, *MPD* main pancreatic duct, *CBD* common bile duct, *GI* gastro-intestinal

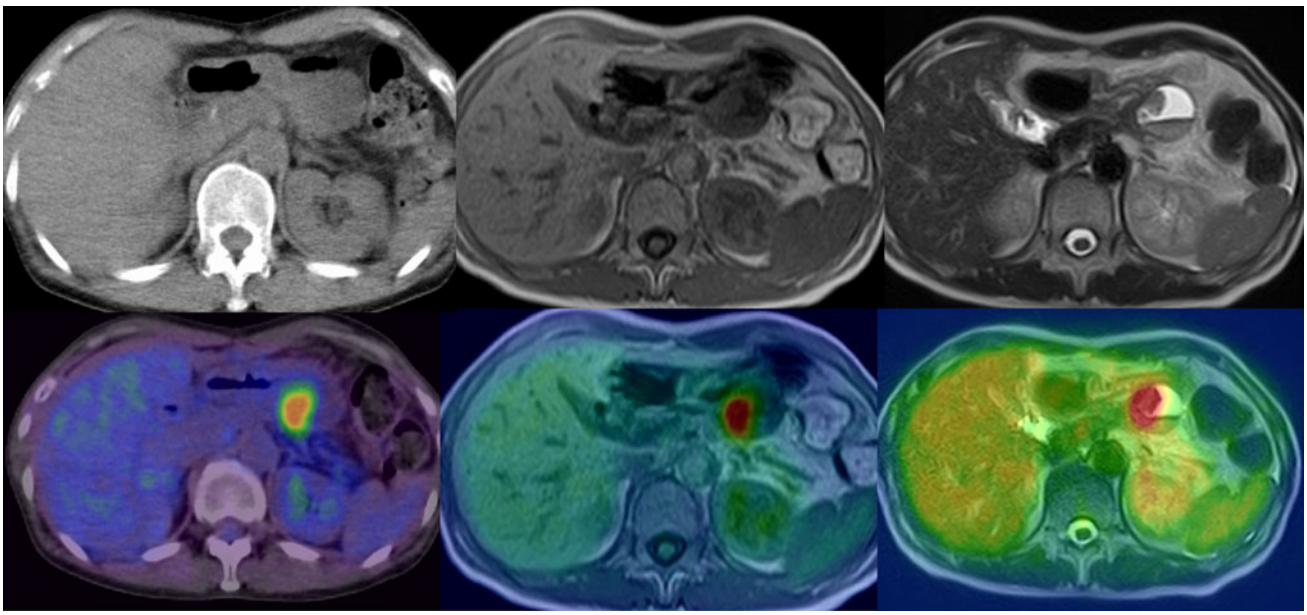

Fig. 1 Low-dose CT showed cystic lesion of pancreas tail (*left upper*). FDG-positive lesion was noted in the cystic tumor by PET/CT (*left lower*). Mural nodule was noted on MRI T1WI (*center upper*). Accordant FDG uptake with mural nodule was noted on PET/MRI-T1 fusion image (*center lower*). Mural nodule in cystic tumor was noted on MRI-T2WI (*right upper*) and FDG uptake accordant with mural nodule was clearly noted by PET/MRI-T2 fusion image (*right lower*). These findings suggested IPMC, which was pathologically proven

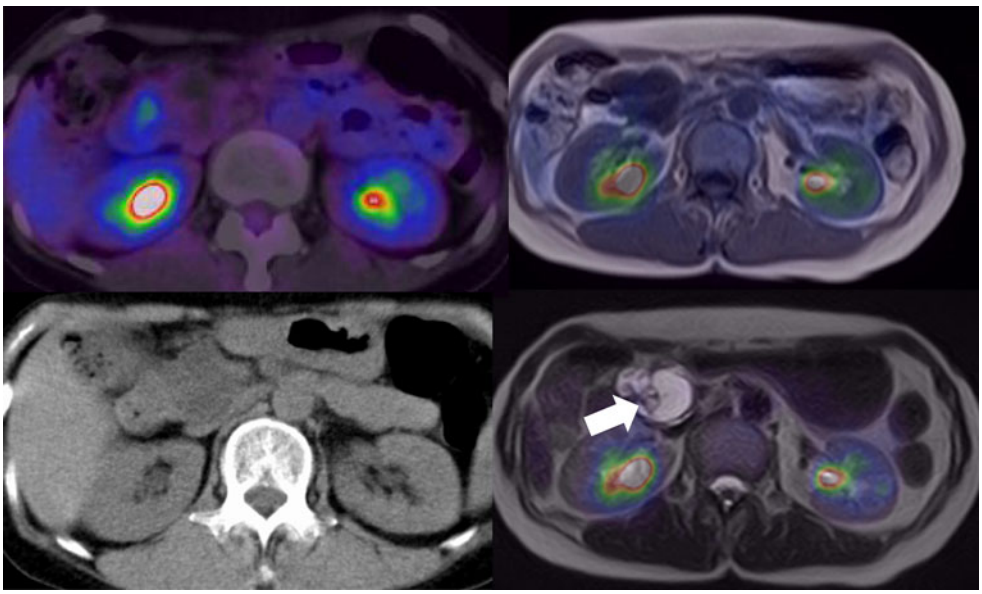

Fig. 2 Low-dose CT (*left lower*) and PET/CT (*left upper*) demonstrated FDG-negative cystic lesion adjacent to duodenum. The case was diagnosed as IPMN by PET/CT. PET/MRI-T1 fusion image showed intra cystic septum without FDG uptake (*right upper*). PET/MRI-T2 fusion image demonstrated FDG-negative mural nodule in the multilocular cystic lesion (*white arrow*), which was suggested to be an intra-ductal papillary mucinous carcinoma (IPMC). The diagnosis was confirmed by surgical operation (*right lower*)

fusion image, and the localized FDG uptake within multilocular structure was confirmed to be malignancy.

Cancer invasion to surrounding vessel, CBD, gastrointestinal tract, or MPD were also detected by PET/MRI fusion image: particularly, MPD obstruction by cancer invasion and dilatation of upper stream were clearly visualized with PET/MRI-T2WI [30] (Fig. 3). In chronic pancreatitis, irregular contour of pancreatic duct is frequently shown. As noted in representative case, MPD showed beaded dilatation and irregularity of ductal contour (Fig. 4). The case was diagnosed as autoimmune pancreatitis during course observation. As for relationship between the tumor and adjacent vessels

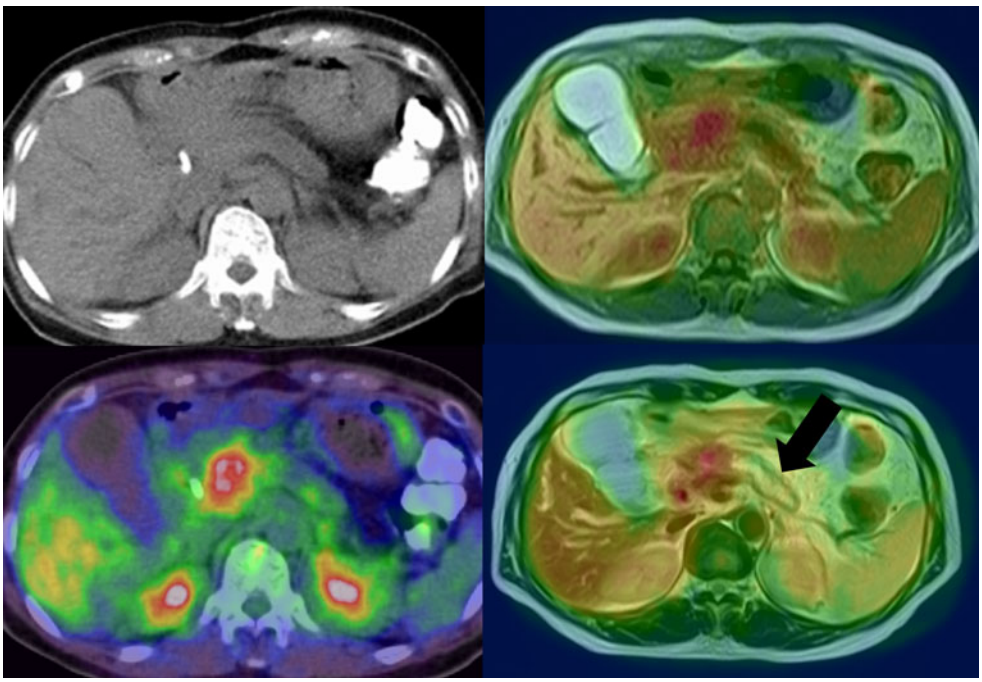

Fig. 3 Although low dose CT did not show any abnormal density area (*left upper*), PET/CT showed intense uptake in accord with pancreatic head cancer (*left lower*). Both PET/MRI-TIWI fusion image (*right upper*) and PET/MRI-T2WI fusion image (*right lower*) demonstrated dilation of MPD (*black arrow*), but PET/MRI-T2WI showed more understandable image

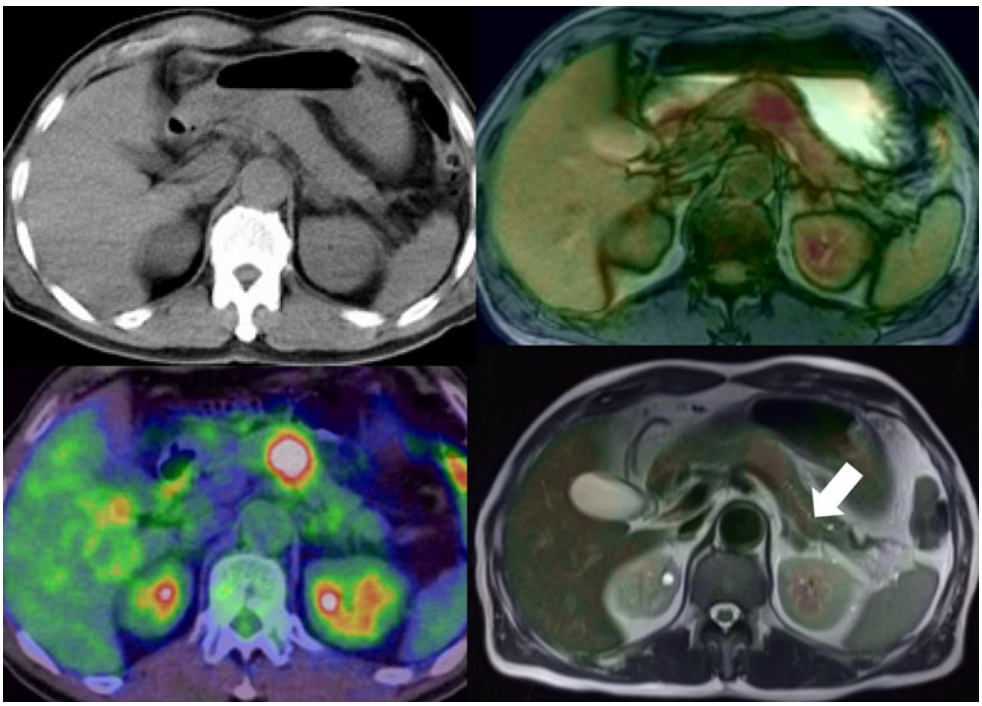

Fig. 4 Low-dose CT showed localized swelling of pancreatic body (*left upper*). Intense FDG uptake was noted in pancreatic body by PET/CT (*left lower*) and the case was considered as pancreas cancer. PET/MRI-T1WI fusion image showed similar information (*right upper*). PET/MRI-T2WI fusion image showed beaded dilatation of pancreatic duct (*white arrow*), which suggested chronic inflammatory change (*right lower*). The case was diagnosed as autoimmune pancreatitis during observation period

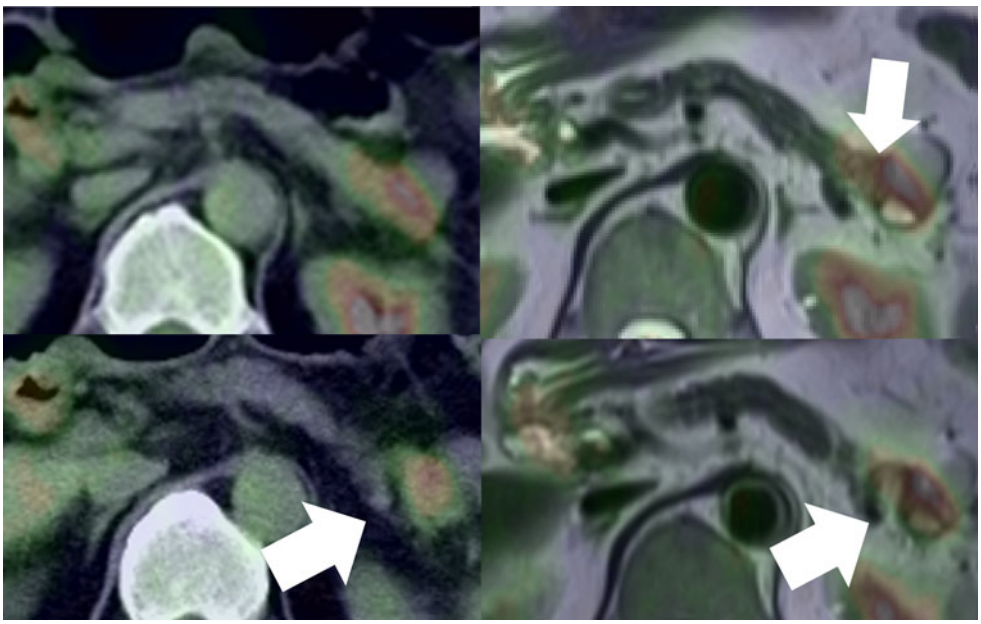

Fig. 5 Although FDG-positive uptake accordant with invasive ductal carcinoma was noted, the relationship with vessel was unclear on PET/CT (*left upper*, *left lower*). In contrast PET/MRI-T2WI (*right upper*, *right lower*) showed that splenic artery was interrupted by FDG uptake tumor, which suggested vascular invasion (*white arrow*). The vessel invasion was pathologically confirmed

like splenic artery, encasement was visualized better by PET/MRI fusion image (Fig. 5). As an additional finding, PET/MRI fusion image could detect additional complicated cysts in almost 10 % in both solid lesion and cystic lesion.

The detectability of invasion was significantly higher in PET/MRI compared with PET/CT, vessels (61.2 vs. 13.4 %), CBD (54.1 vs. 10.8 %), and GI tract (29.8 vs. 10.6 %) respectively (Table 5).

Discussion

The current study demonstrated that PET/MRI fusion image gave better diagnostic performance compared with that of FDG-PET/CT in the differentiation of pancreatic cancer. Twelve of 119 cases (10.0 %) were accurately diagnosed based only on morphological diagnosis by PET/MRI.

Diagnosing solid type pancreatic cancer becomes easy when typical finding like irregular shaped low-density mass is noted on computed tomography (CT) [31]. However, in diagnosing CT without contrast-media, cancer is easily overlooked if tumor has the similar density like normal pancreatic tissue [22]. In such cases, high FDG uptake in accordance with mass lesion is the diagnostic finding suggesting pancreatic cancer [1, 6, 7, 9, 10, 32]. However, inflammatory cells also show increased FDG uptake because of accelerated glucose metabolism; therefore, the differential diagnosis between active pancreatitis and cancer is difficult [1]. In general, FDG uptake pattern was often noted as diffuse uptake in AIP [4]. Nevertheless, when AIP appeared as focal mass persistently it can be mistaken for pancreatic cancer [9, 11, 33]. Although the diagnostic sensitivity of PET/CT in solid lesion was superior to previous report [10], its accuracy was not so good because we could not differentiate non-calcified chronic pancreatitis from pancreatic cancer. In this respect, indirect diagnostic valuable findings were helpfully added by PET/MRI fusion image. Particularly, finding of main pancreatic duct (MPD), such as dilation of caudal side when cancer invades MPD, was useful information [34]. Although there are some exceptions [35], it is a reliable diagnostic finding for differential diagnosis [30]. In chronic pancreatitis, moderately tortuous dilatation and irregularity of MPD, so called Beads-forming dilatation of MPD, is noted [34]. However, even if spindly contour or disruption of MPD is seen, no dilatation of upstream side is noted [34]. In the current study, PET/MRI fusion images provided diagnostic findings such as non-dilated MPD within high FDG uptake of pancreatic mass, which suggested mass-forming pancreatitis. In addition, beaded dilation of MPD which was not precisely shown by low-dose plain CT was also visualized clearly by PET/MRI fusion images. Diffuse enlargement of the pancreas and effacement of the lobular contour of the pancreas, the so-called "sausage-like" appearance, a typical finding of AIP [36, 37], was also more clearly depicted by PET/MRI fusion images. Thus diagnostic accuracy was improved significantly in solid lesions.

Both ^{18}F-FDG-PET and ^{18}F-FDG-PET/CT are useful for differential diagnosis in various cystic pancreas tumor [2, 9, 38, 39]. Among these tumors, the correct diagnosis of IPNM is very important because it is a slow-growing tumor with hyperplasia-adenoma-carcinoma sequence pathologically [40]. Multilocular cystic mass with large tumor

Table 5 Comparison of detectability of peri-pancreatic invasion by PET/CT and PET/MRI fusion images pancreas cancer

	PET/CT	PET/MRI
Invasion of adjacent vessels ($n = 67$)	9 (13.4)	41 (61.2)*
Invasion of CBD ($n = 37$)	4 (10.8)	20 (54.1)*
Invasion into GI tract ($n = 47$)	5 (10.6)	14 (29.8)*
		(%)

CBD common bile duct, *GI* gastro-intestinal

* $P < 0.01$

diameter and intense FDG uptake can be easily diagnosed as malignant cystic tumor [38]. However, there are some overlaps of FDG uptake between benign cystic lesions and malignant cystic tumors [2]. In this respect, MRI is beneficial in diagnosing cystic mass precisely by visualizing solid component such as mural nodule or capsule structure [34, 41–44]. We could demonstrate both multi-locular structures and mural nodule clearly by fusion PET/MRI-T2 images in the current study. However, the statistical significance was not noted between PET/CT and PET/MRI fusion images in the current study. The possible reason was that few malignant cystic tumor cases had FDG-negative intramural nodule. In addition, no patients of false-positive cases such as inflammatory cystic lesions were included, either. We should recheck the statistical significance by analyzing more patients with cystic lesions having mural nodule.

It is extremely important to diagnose cancer invasion of peri-pancreatic tissues. The most important preoperative factor for resectability is vascular invasion into superior mesenteric artery (SMA) or celiac artery [24], which is very difficult to determine using FDG-PET [45]. In general, vascular invasions are diagnosed based on extensive circumferential contact between cancer and vessels, occlusion of vessels, or the mass effect of one side of the vessel [24–26]. Low-dose CT can evaluate vessels, but it is sometimes unfeasible owing to limited density resolution. In contrast, MRI has an excellent diagnostic ability to detect vascular invasion [24]. In the current study, encasements of major vessels such as gastro-colic trunk or splenic vein were better visualized with PET/MRI-T2 fusion images in about the half of solid type cancers, which suggested unresectability or altered surgical strategy.

Although reliable imaging method for diagnosing cancer invasion into extra-pancreatic nerve plexus (PLX) has not been established, it is one of the important issues in choosing treatment strategy and predicting prognosis [46, 47]. Streaky and strand-like signal intensity structures in fat tissue, using MRI, have been used to diagnose PLX invasion [46]. In the current study, some of the advanced pancreatic cancer cases showed streak-like structure with intense FDG uptake suggesting PLX invasion, but it was not confirmed surgically. Future analyses with larger numbers of patients need to be conducted in resolving the problem.

As an additional finding, cystic lesions such as pseudocyst or retention cyst due to obstruction of MPD are sometimes found in pancreas cancer or pancreatitis [42, 48]. In the current study, PET/MRI-T2 fusion image detected them unexpectedly in about 10 % of cases.

The current study has some limitations. First, fusion-images were made retrospectively by paired images taken at a few days' intervals. Therefore, misregistration of PET and MRI image due to dislocation of organs between two examinations was unavoidable.

The second limitation was that used T1WI for the fusion was without fat-suppression. Because fat-suppression T1WI can delineate contour of pancreas better, FDG-PET/fat-suppression T1W fusion image may have accomplished better diagnosability in evaluating vascular encasement or CBD invasion. In our retrospective analyses, we used T1WI without fat-suppression for PET/MRI fusion because some of the current cases did not choose fat-suppression T1. This limitation caused disadvantageous results to PET/T1 MRI fusion images compared with PET/MRI T2 images in assessing peri-pancreatic invasion. Future studies should be evaluated with FDG-PET/fat-suppression T1WI MRI fusion.

Conclusion

Regarding pancreatic tumor, FDG-PET/MRI fusion image proved to be useful in differentiating pancreatic cancer from benign lesion although the statistically significant difference was confirmed only in solid lesions.

In addition, the relationship with the surrounding or internal structures such as blood vessels, bile duct system, and pancreatic duct became more apparent, thus helping evaluate cancer invasion and detect other benign cystic lesions as well.

References

1. Murakami K. FDG-PET for hepatobiliary and pancreatic cancer: advances and current limitations. World J Clin Oncol. 2011;2:229–36.
2. Takanami K, Hiraide T, Tsuda M, Nakamura Y, Kaneta T, Takase K, et al. Additional value of FDG PET/CT to contrast-enhanced CT in the differentiation between benign and malignant intraductal papillary mucinous neoplasms of the pancreas with mural nodules. Ann Nucl Med. 2011;25:501–10.
3. Berberat P, Friess H, Kashiwagi M, Beger HG, Buchler MW. Diagnosis and staging of pancreatic cancer by positron emission tomography. World J Surg. 1999;23:882–7.

4. Nakamoto Y, Saga T, Ishimori T, Higashi T, Mamede M, Okazaki K, et al. FDG-PET of autoimmune-related pancreatitis: preliminary results. Eur J Nucl Med. 2000;27:1835–8.
5. Okano K, Kakinoki K, Akamoto S, Hagiike M, Usuki H, Yamamoto Y, et al. 18F-fluorodeoxyglucose positron emission tomography in the diagnosis of small pancreatic cancer. World J Gastroenterol. 2011;17:231–5.
6. Lyshchik A, Higashi T, Nakamoto Y, Fujimoto K, Doi R, Imamura M, et al. Dual-phase 18F-fluoro-2-deoxy-D-glucose positron emission tomography as a prognostic parameter in patients with pancreatic cancer. Eur J Nucl Med Mol Imaging. 2005;32:389–97.
7. Friess H, Langhans J, Ebert M, Beger HG, Stollfuss J, Reske SN, et al. Diagnosis of pancreatic cancer by 2[18F]-fluoro-2-deoxy-D-glucose positron emission tomography. Gut. 1995;36:771–7.
8. Stollfuss JC, Glatting G, Friess H, Kocher F, Berger HG, Reske SN. 2-(fluorine-18)-fluoro-2-deoxy-D-glucose PET in detection of pancreatic cancer: value of quantitative image interpretation. Radiology. 1995;195:339–44.
9. Higashi T, Saga T, Nakamoto Y, Ishimori T, Fujimoto K, Doi R, et al. Diagnosis of pancreatic cancer using fluorine-18 fluorodeoxyglucose positron emission tomography (FDG PET)—usefulness and limitations in "clinical reality". Ann Nucl Med. 2003; 17:261–79.
10. Schick V, Franzius C, Beyna T, Oei ML, Schnekenburger J, Weckesser M, et al. Diagnostic impact of 18F-FDG PET-CT evaluating solid pancreatic lesions versus endosonography, endoscopic retrograde cholangio-pancreatography with intraductal ultrasonography and abdominal ultrasound. Eur J Nucl Med Mol Imaging. 2008;35:1775–85.
11. Nguyen VX, Nguyen CC, Nguyen BD. (18)F-FDG PET/CT imaging of the pancreas: spectrum of diseases. J Pancreas 2011; 12:557–66.
12. Nagamachi S, Wakamatsu H, Kiyohara S, Fujita S, Futami S, Arita H, et al. Usefulness of a deep-inspiration breath-hold 18F-FDG PET/CT technique in diagnosing liver, bile duct, and pancreas tumors. Nucl Med Commun. 2009;30:326–32.
13. Mergo PJ, Helmberger TK, Buetow PC, Helmberger RC, Ros PR. Pancreatic neoplasms: mR imaging and pathologic correlation. Radiographics. 1997;17:281–301.
14. Schlemmer HP, Pichler BJ, Krieg R, Heiss WD. An integrated MR/PET system: prospective applications. Abdom Imaging. 2009;34:668–74.
15. Schwenzer NF, Schraml C, Muller M, Brendle C, Sauter A, Spengler W, et al.: Pulmonary lesion assessment: comparison of whole-body hybrid MR/PET and PET/CT imaging—pilot study. Radiology. 2012;264:551–8.
16. Drzezga A, Souvatzoglou M, Eiber M, Beer AJ, Furst S, Martinez-Moller A, et al. first clinical experience with integrated whole-body PET/MR: comparison to PET/CT in patients with oncologic diagnoses. J Nucl Med. 2012;53:845–55.
17. Donati OF, Hany TF, Reiner CS, von Schulthess GK, Marincek B, Seifert B, et al. Value of retrospective fusion of PET and MR images in detection of hepatic metastases: comparison with 18F-FDG PET/CT and Gd-EOB-DTPA-enhanced MRI. J Nucl Med. 2010;51:692–9.
18. Nakajo K, Tatsumi M, Inoue A, Isohashi K, Higuchi I, Kato H, et al. Diagnostic performance of fluorodeoxyglucose positron emission tomography/magnetic resonance imaging fusion images of gynecological malignant tumors: comparison with positron emission tomography/computed tomography. Jpn J Radiol. 2010;28:95–100.
19. Ruf J. Lopez Hanninen E, Bohmig M, Koch I, Denecke T, Plotkin M, et al.: Impact of FDG-PET/MRI image fusion on the detection of pancreatic cancer. Pancreatology. 2006;6:512–9.
20. Tatsumi M, Isohashi K, Onishi H, Hori M, Kim T, Higuchi I, et al. 18F-FDG PET/MRI fusion in characterizing pancreatic tumors: comparison to PET/CT. Int J Clin Oncol. 2011;16:408–15.
21. Miller FH, Keppke AL, Wadhwa A, Ly JN, Dalal K, Kamler VA. MRI of pancreatitis and its complications: part 2, chronic pancreatitis. Am J Roentgenol. 2004;183:1645–52.
22. Ros PR, Mortele KJ. Imaging features of pancreatic neoplasms. JBR-BTR. 2001;84:239–49.
23. Vitellas KM, Keogan MT, Spritzer CE, Nelson RC. MR cholangiopancreatography of bile and pancreatic duct abnormalities with emphasis on the single-shot fast spin-echo technique. Radiographics. 2000;20:939–57.
24. Buchs NC, Chilcott M, Poletti PA, Buhler LH, Morel P. Vascular invasion in pancreatic cancer: imaging modalities, preoperative diagnosis and surgical management. World J Gastroenterol. 2010;16:818–31.
25. Lu DS, Reber HA, Krasny RM, Kadell BM, Sayre J. Local staging of pancreatic cancer: criteria for unresectability of major vessels as revealed by pancreatic-phase, thin-section helical CT. Am J Roentgenol. 1997;168:1439–43.
26. Nakayama Y, Yamashita Y, Kadota M, Takahashi M, Kanemitsu K, Hiraoka T, et al. Vascular encasement by pancreatic cancer: correlation of CT findings with surgical and pathologic results. J Comput Assist Tomogr. 2001;25:337–42.
27. Li H, Zeng MS, Zhou KR, Jin DY, Lou WH. Pancreatic adenocarcinoma: the different CT criteria for peripancreatic major arterial and venous invasion. J Comput Assist Tomogr. 2005;29: 170–5.
28. Arakawa A, Yamashita Y, Namimoto T, Tang Y, Tsuruta J, Kanemitsu K, et al. Intraductal papillary tumors of the pancreas. Histopathologic correlation of MR cholangiopancreatography findings. Acta Radiol. 2000;41:343–7.
29. Lopez HE, Amthauer H, Hosten N, Ricke J, Bohmig M, Langrehr J, et al. Prospective evaluation of pancreatic tumors: accuracy of MR imaging with MR cholangiopancreatography and MR angiography. Radiology. 2002;224:34–41.
30. Irie H, Honda H, Aibe H, Kuroiwa T, Yoshimitsu K, Shinozaki K, et al. MR cholangiopancreatographic differentiation of benign and malignant intraductal mucin-producing tumors of the pancreas. AJR Am J Roentgenol. 2000;174:1403–8.
31. Ardengh JC, Goldman SM, de Lima-Filho ER. Current role of imaging methods in the diagnosis of cystic solid pancreas neoplasms: part II. Rev Col Bras Cir. 2011;38:192–7.
32. Zimny M, Schumpelick V. Fluorodeoxyglucose positron emission tomography (FDG-PET) in the differential diagnosis of pancreatic lesions. Chirurg. 2001;72:989–94.
33. Sahani DV, Sainani NI, Deshpande V, Shaikh MS, Frinkelberg DL. Fernandez-del Castillo C: Autoimmune pancreatitis: disease evolution, staging, response assessment, and CT features that predict response to corticosteroid therapy. Radiology. 2009;250:118–29.
34. Hakime A, Giraud M, Vullierme MP, Vilgrain V. MR imaging of the pancreas. J Radiol. 2007;88:11–25.
35. Sugiyama M, Izumisato Y, Abe N, Masaki T, Mori T, Atomi Y. Pancreatic carcinoma that completely obstructs the Wirsung duct without dilatation of the main pancreatic duct. J Gastroenterol Hepatol. 2006;21:1154–6.
36. Takuma K, Kamisawa T, Gopalakrishna R, Hara S, Tabata T, Inaba Y, et al. Strategy to differentiate autoimmune pancreatitis from pancreas cancer. World J Gastroenterol. 2012;18:1015–20.
37. Sahani DV, Kalva SP, Farrell J, Maher MM, Saini S, Mueller PR, et al. Autoimmune pancreatitis: imaging features. Radiology. 2004;233:345–52.
38. Fischer MA, Donati O, Heinrich S, Weber A, Hany TF, Soldini D, et al. Intraductal oncocytic papillary neoplasm of the pancreas: a radio-pathological case study. J Pancreas. 2010;11:49–54.

39. Sperti C, Pasquali C, Chierichetti F, Liessi G, Ferlin G, Pedrazzoli S. Value of 18-fluorodeoxyglucose positron emission tomography in the management of patients with cystic tumors of the pancreas. Ann Surg. 2001;234:675–80.
40. Baiocchi GL, Portolani N, Bertagna F, Gheza F, Pizzocaro C, Giubbini R, et al. Possible additional value of 18FDG-PET in managing pancreas intraductal papillary mucinous neoplasms: preliminary results. J Exp Clin Cancer Res. 2008;27:10.
41. Ku YM, Shin SS, Lee CH, Semelka RC. Magnetic resonance imaging of cystic and endocrine pancreatic neoplasms. Top Magn Reson Imaging. 2009;20:11–8.
42. Kalb B, Sarmiento JM, Kooby DA, Adsay NV, Martin DR. MR imaging of cystic lesions of the pancreas. Radiographics. 2009;29:1749–65.
43. Pilleul F, Rochette A, Partensky C, Scoazec JY, Bernard P, Valette PJ. Preoperative evaluation of intraductal papillary mucinous tumors performed by pancreatic magnetic resonance imaging and correlated with surgical and histopathologic findings. J Magn Reson Imaging. 2005;21:237–44.
44. Schima W. MRI of the pancreas: tumours and tumour-simulating processes. Cancer Imaging. 2006;6:199–203.
45. Izuishi K, Yamamoto Y, Sano T, Takebayashi R, Masaki T, Suzuki Y. Impact of 18-fluorodeoxyglucose positron emission tomography on the management of pancreatic cancer. J Gastrointest Surg. 2010;14:1151–8.
46. Zhang XM, Mitchell DG, Witkiewicz A, Verma S, Bergin D. Extrapancreatic neural plexus invasion by pancreatic carcinoma: characteristics on magnetic resonance imaging. Abdom Imaging. 2009;34:634–41.
47. Mochizuki K, Gabata T, Kozaka K, Hattori Y, Zen Y, Kitagawa H, et al. MDCT findings of extrapancreatic nerve plexus invasion by pancreas head carcinoma: correlation with en bloc pathological specimens and diagnostic accuracy. Eur Radiol. 2010;20:1757–67.
48. Inagi E, Shimodan S, Amizuka H, Kigawa S, Shimizu Y, Nagashima K, et al. Pancreatic cancer initially presenting with a pseudocyst at the splenic flexure. Pathol Int. 2006;56:558–62.